Conservation of Complex Power Technique for Waveguide Junctions with Finite Wall Conductivity

J. DOUGLAS WADE, MEMBER, IEEE, AND ROBERT H. MACPHIE, SENIOR MEMBER, IEEE

Abstract—Scattering at the junction of two waveguides with finite wall conductivity is rigorously treated using E-field mode matching and the conservation of complex power technique. At the transverse junction discontinuity between the two waveguides the complex power absorbed by the junction wall is taken into account along with the usual transfer of complex power from one guide to the other. This leads to a generalized form of the scattering matrix $[S]$ of the lossy junction which incorporates the surface impedance Z_m of the transverse metallic wall, assumed to be a good conductor. The specific case of a copper transverse diaphragm with centered circular iris in X-band guide is considered and the equivalent TE_{10} shunt admittance is computed. Numerical results are also given for lossy X-band cavity resonators with circular coupling holes.

I. INTRODUCTION

IN RECENT YEARS a considerable number of waveguide scattering problems have been successfully handled in a rigorous fashion by combining mode matching of the transverse electric fields at a given waveguide junction with enforcement of the conservation of complex power at the same discontinuity [1]–[3]. This conservation of complex power technique (CCPT) has, in particular, provided a formally exact solution to the problem of scattering at circular-to-rectangular waveguide junctions and to the related problem of scattering at a thick diaphragm with a circular coupling hole in a rectangular waveguide [4].

However, in this and all earlier work, the walls of both the waveguides themselves and of the transverse discontinuities, e.g. diaphragms, were assumed to be *perfectly conducting*. This is quite valid for a large number of cases such as simple junctions between waveguides of different cross sections or at single diaphragms. For good conductors (copper, silver) the scattering matrices of such configurations would be virtually identical to those for the idealized perfectly conducting case. For cavity resonators and filters, however, the wall losses on both the end plates and on the waveguide walls themselves are significant.

It is the purpose of this paper to extend the conservation of complex power technique to include the effects of the conductivity of the metal from which such waveguide components are fabricated. Particular attention will be paid to the circular-to-rectangular waveguide junction problems treated in [4] for the lossless case, but the generalization is valid for virtually any problem which can be treated by the original conservation of complex power technique.

Manuscript received August 24, 1989; revised November 21, 1989. This work was supported by the Natural Sciences and Engineering Research Council of Canada under Grant A-2176.
J. D. Wade is with the National Research Council's Herzberg Institute for Astrophysics in Ottawa, Ont., Canada K1A 0R6.
R. H. MacPhie is with the Electrical Engineering Department, University of Waterloo, Waterloo, Ont., Canada N2L 3G1.
IEEE Log Number 8933716.

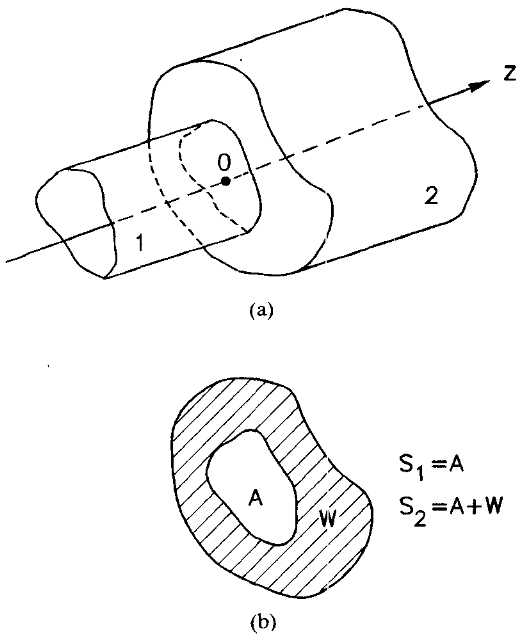

Fig. 1. (a) The junction of two waveguides. (b) The junction plane at $z=0$.

II. MODAL EXPANSIONS OF THE FIELDS

Consider a junction of two waveguides at $z=0$, as shown in Fig. 1. In guide 1 the transverse electric and magnetic fields at $z=0_-$ can be written as

$$E_{t1}=\sum_n (a_n^+ + a_n^-)e_{1n} \tag{1}$$

$$H_{t1}=\sum_n (a_n^+ - a_n^-)Y_{1n}z\times e_{1n}. \tag{2}$$

Similarly, in guide 2, just to the right of the junction at

0018-9480/90/0400-0373$01.00 ©1990 IEEE

$z = 0_+$, we have

$$\boldsymbol{E}_{t2} = \sum_q (c_q^- + c_q^+) \boldsymbol{e}_{2q} \tag{3}$$

$$\boldsymbol{H}_{t2} = \sum_q (c_q^- - c_q^+) Y_{2q} \hat{z} \times \boldsymbol{e}_{2q}. \tag{4}$$

In (1)–(4) a time dependence of $\exp(j\omega t)$ is assumed and + and − indicate waves which are incident on and reflected from the junction respectively. The vector functions $\boldsymbol{e}_{1n}$ and $\boldsymbol{e}_{2q}$ are the transverse modal E fields (TE and/or TM) in guides 1 and 2 respectively, and the modal admittances are

$$Y_{im} = \begin{cases} \dfrac{\gamma_{im}}{j\omega\mu_i} & \text{(TE modes)} \\ \dfrac{j\omega\epsilon_i}{\gamma_{im}} & \text{(TM modes)} \end{cases} \tag{5}$$

for $m = 1, 2, 3, \cdots$ and $i = 1, 2$.

In this paper we assume that the losses are due to wall conductivity and so the permeability μ_i and permittivity ϵ_i in (5) are both real. The modal propagation constant γ_{im} is complex due to the wall losses.

However, we will make the reasonable assumption that the wall losses are relatively small and that the E-field modes are real and orthonormal:

$$\int_{S_i} \boldsymbol{e}_{im} \cdot \boldsymbol{e}_{in}\, ds = \delta_{mn} = \begin{cases} 1, & m = n \\ 0, & m \neq n \end{cases} \tag{6}$$

where the integration is over the cross section S_i of the ith guide.

The various modal amplitudes $a_n^{\pm}$ and $c_m^{\pm}$ in (1)–(4) are related by means of the modal scattering matrix $[S]$ of the junction. In matrix notation

$$\begin{bmatrix} \underline{a}^- \\ \underline{c}^- \end{bmatrix} = \begin{bmatrix} [S_{11}] & [S_{12}] \\ [S_{21}] & [S_{22}] \end{bmatrix} \begin{bmatrix} \underline{a}^+ \\ \underline{c}^+ \end{bmatrix} \tag{7}$$

where $\underline{a}^{\pm}$ and $\underline{c}^{\pm}$ denote column matrices whose nth and mth elements are $a_n^{\pm}$ and $c_m^{\pm}$ respectively.

III. E-Field Matching at the Junction

At the junction ($z = 0$) the transverse E field of the larger guide 2 must satisfy

$$\boldsymbol{E}_{t2} = \begin{cases} \boldsymbol{E}_{t1} & \text{(in aperture } A) \\ Z_m \hat{z} \times \boldsymbol{H}_{t2} & \text{(on wall } W) \end{cases} \tag{8}$$

where, for a good conductor, the surface impedance of the transverse wall W is

$$Z_m = (1 + j)\sqrt{\frac{\omega\mu_0}{2\sigma}} \tag{9}$$

with σ being the conductivity of the wall metal.

Substituting (1), (3), and (4) into (8), scalar multiplying by $\boldsymbol{e}_{2m}$, and integrating over S_2 we obtain

$$\sum_q (c_q^- + c_q^+) \int_{S_2} \boldsymbol{e}_{2q} \cdot \boldsymbol{e}_{2m}\, ds = \sum_n (a_n^+ + a_n^-) \int_A \boldsymbol{e}_{1n} \cdot \boldsymbol{e}_{2m}\, ds - Z_m \sum_q (c_q^- - c_q^+) Y_{2q} \int_W \boldsymbol{e}_{2q} \cdot \boldsymbol{e}_{2m}\, ds. \tag{10}$$

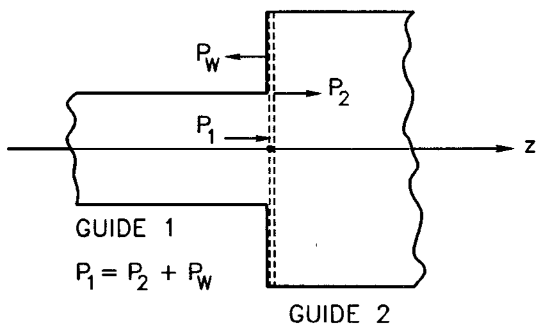

Fig. 2. Conservation of complex power at the junction of two waveguides.

Due to mode orthogonality this simplifies to

$$c_m^- + c_m^+ = \sum_n M_{mn} (a_n^+ + a_n^-) + Z_m \sum_q W_{mq} Y_{2q} (c_q^+ - c_q^-) \tag{11}$$

where

$$M_{mn} = \int_A \boldsymbol{e}_{2m} \cdot \boldsymbol{e}_{1n}\, ds, \qquad W_{mq} = \int_W \boldsymbol{e}_{2m} \cdot \boldsymbol{e}_{2q}\, ds. \tag{12}$$

In matrix notation we can rewrite (11) as follows:

$$\underline{c}^+ + \underline{c}^- = [M](\underline{a}^+ + \underline{a}^-) + Z_m [W][Y_2](\underline{c}^+ - \underline{c}^-) \tag{13}$$

where $[Y_2]$ is the modal admittance matrix of guide 2, which for low losses we will assume is diagonal.

IV. Conservation of Complex Power at the Junction

With reference to Fig. 2, the complex power P_1 passing from guide 1 must be equal to the complex power P_2 flowing into guide 2 plus the complex power P_W flowing into the wall W.

In guide 1 we have

$$P_1 = \int_{S_1} \boldsymbol{E}_1 \times \boldsymbol{H}_1^* \cdot ds \tag{14}$$

and using (1) and (2) at $z = 0_-$ we easily obtain

$$P_1 = (\underline{a}^+ - \underline{a}^-)^{\dagger} [Y_1]^{\dagger} (\underline{a}^+ + \underline{a}^-) \tag{15}$$

where † indicates the Hermitian transpose operator ($[A]^{\dagger} = [A^*]^T$ where T is the transpose operator).

Likewise in guide 2,

$$P_2 = (\underline{c}^- - \underline{c}^+)^{\dagger} [Y_2]^{\dagger} (\underline{c}^+ + \underline{c}^-). \tag{16}$$

Moreover, the wall power can be written as

$$P_W = Z_m \int_W \boldsymbol{H}_2 \cdot \boldsymbol{H}_2^*\, ds \tag{17}$$

and using (4) and (12) we obtain

$$P_W = Z_m (\underline{c}^- - \underline{c}^+)^{\dagger} [Y_2]^{\dagger} [W][Y_2] (\underline{c}^- - \underline{c}^+). \tag{18}$$

Conservation of complex power dictates that

$$P_1 = P_2 + P_W \tag{19}$$

and in view of (15), (16), and (18) we can write

$$(\underline{a}^+ - \underline{a}^-)^\dagger [Y_1]^\dagger (\underline{a}^+ + \underline{a}^-) = (\underline{c}^- - \underline{c}^+)^\dagger \{[Y_2]^\dagger (\underline{c}^- + \underline{c}^+) + Z_m [Y_2]^\dagger [W][Y_2](\underline{c}^- - \underline{c}^+)\}. \tag{20}$$

Using (20), together with the E-field mode matching equation (13), it is easy to show that

$$[M]^T [Y_2](\underline{c}^- - \underline{c}^+) = [Y_1](\underline{a}^+ - \underline{a}^-) \tag{21}$$

which, effectively, is the equation for H-field matching over the aperture A only.

V. The Scattering Matrix $[S]$ of the Lossy Junction

If we assume that there is energy incident on the junction from guide 1 only, then $\underline{c}^+ = 0$ in (13) and (21). Moreover, it is shown in the Appendix that

$$[W] = [I] - [M][M]^T \tag{22}$$

and as a result (13) and (21) become

$$\underline{c}^- = [M](\underline{a}^+ + \underline{a}^-) - Z_m[Y_2]\underline{c}^- + Z_m[M][M]^T[Y_2]\underline{c}^- \tag{23}$$

and

$$[M]^T[Y_2]\underline{c}^- = [Y_1](\underline{a}^+ - \underline{a}^-). \tag{24}$$

Using (24) and (23) and defining an admittance matrix

$$[Y_L] = [M]^T[Y_2]([I] + Z_m[Y_2])^{-1}[M] \tag{25}$$

we can, after some algebra, show that

$$\underline{a}^- = ([Y_1] - Z_m[Y_L][Y_1] + [Y_L])^{-1} \cdot ([Y_1] - Z_m[Y_L][Y_1] - [Y_L])\underline{a}^+. \tag{26}$$

But with $\underline{c}^+ = 0$, and in view of (7) it follows that

$$[S_{11}] = ([Y_1] - Z_m[Y_L][Y_1] + [Y_L])^{-1} \cdot ([Y_1] - Z_m[Y_L][Y_1] - [Y_L]). \tag{27}$$

As in the lossless case ([1], [2]), we will now use the E-field mode matching equation (23) to deduce $[S_{21}]$ in terms of $[S_{11}]$. Simple algebra leads to

$$[S_{21}] = ([I] + Z_m[Y_2])^{-1} \cdot [M]([I] + Z_m[Y_1] + ([I] - Z_m[Y_1])[S_{11}]). \tag{28}$$

A similar process whereby we assume that incidence is from guide 2, with $\underline{a}^+ = 0$, permits us to obtain matrix expressions for $[S_{12}]$ and $[S_{22}]$:

$$[S_{12}] = 2([Y_1] + [Y_L]([I] - Z_m[Y_1]))^{-1} \cdot [M]^T[Y_2]([I] + Z_m[Y_2])^{-1} \tag{29}$$

$$[S_{22}] = ([I] + Z_m[Y_2])^{-1} \cdot ([M]([I] - Z_m[Y_1])[S_{12}] - ([I] + Z_m[Y_2])). \tag{30}$$

Of course, in the case of a perfectly conducting wall $Z_m \to 0$ and (28)–(30) simplify to more familiar [4, p. 1088] expressions:

$$[S_{11}] = ([Y_1] + [Y_{L1}])^{-1}([Y_1] - [Y_{L1}]), \quad [S_{21}] = [M]([I] + [S_{11}]) \tag{31}$$

$$[S_{12}] = 2([Y_1] + [Y_2])^{-1}[M][Y_2], \quad [S_{22}] = [M][S_{12}] - [I] \tag{32}$$

where

$$[Y_{L1}] = [M]^T[Y_2][M]. \tag{33}$$

Another limiting case is that of a lossy short-circuiting plate ($A \to 0$, $W \to S_2$). In this case $[M] = 0$ and only $[S_{22}]$ is nonzero:

$$[S_{22}] = ([I] + Z_m[Y_2])^{-1}([Z_m][Y_2] - [I]) \tag{34}$$

and if $Z_m \to 0$, then $[S_{22}] = -[I]$, as expected.

VI. The Effects of Waveguide Wall Losses

In Section VII we will treat the cases of rectangular one- and two-port cavity resonators with losses not only in the transverse diaphragms and end plates but also in the walls of the waveguide themselves. With such losses, not only do the modal propagation constants become complex but, in principle, the modes themselves become coupled [5, pp. 126–129]. A more detailed discussion is provided by Gustincic [6]. But rather than proceeding in this direction we will assume that the walls are very good conductors and that the cross-coupling of the modal powers is negligible.

Moreover, only the dominant TE_{10} mode will be propagating and we will assume that the waveguide wall losses are due only to this mode since it has the largest amplitude, especially for high-Q cavities with small coupling holes. Consequently, in the generalized scattering matrix formulas [2], [3] used to calculate the overall scattering matrix $[S_c]$ of a cascade of two or more transverse junctions, it will be assumed that the TE_{10} mode has a complex propagation constant $\gamma_{10}^{TE} = \alpha_{10}^{TE} + j\beta_{10}^{TE}$ and all other cutoff modes have real propagation constants. For a rectangular guide of width a and height b,

$$\beta_{10}^{TE} = \sqrt{\omega^2\mu\epsilon - \left(\frac{\pi}{a}\right)^2} \tag{35}$$

$$\alpha_{10}^{TE} = \frac{2b\left(\frac{\pi}{a}\right)^2 + a\omega^2\mu\epsilon}{ab\beta_{10}^{TE}\sqrt{2\omega\mu\sigma}} \tag{36}$$

if $\alpha_{10}^{TE} \ll \beta_{10}^{TE}$.

VII. Lossy Rectangular Cavities with Circular Coupling Holes

In a previous paper [4] the authors considered the case of scattering at *lossless* circular-to-rectangular waveguide junctions, in particular a thin diaphragm with a centered

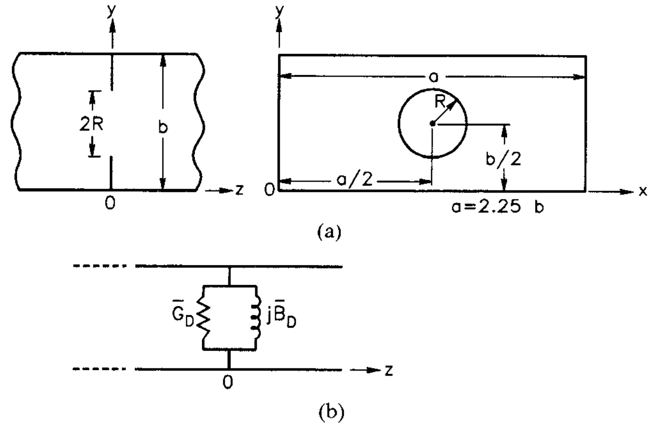

Fig. 3. (a) Thin diaphragm with centered circular hole in rectangular waveguide. (b) The equivalent transmission line circuit.

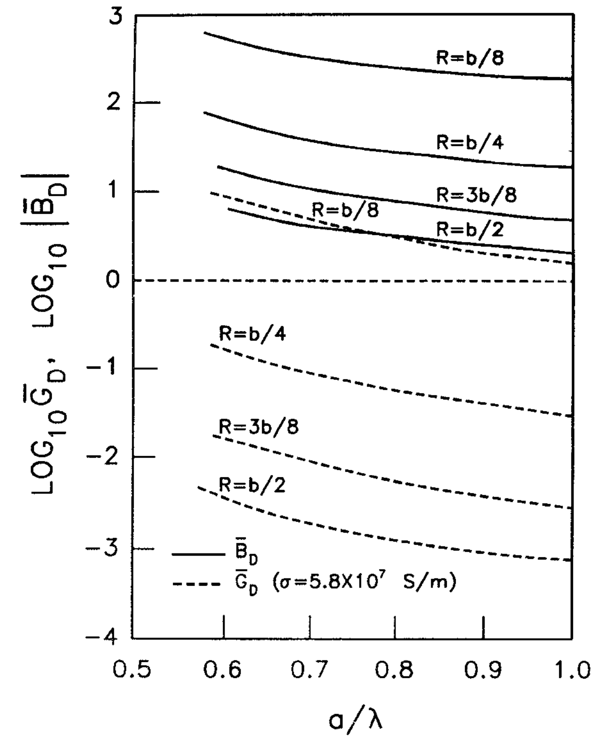

Fig. 4. Equivalent shunt admittance (normalized) of a thin lossy diaphragm with a centered circular hole in X-band waveguide.

circular hole in rectangular guide. Before dealing with cavities, let us consider the effect of wall losses on the equivalent admittance of such a diaphragm (illustrated in Fig. 3). Using the generalized scattering matrix technique as described in [4] but with the various component matrices now generalized to include wall losses, as specified by (27)–(30), a computer program was developed to calculate the equivalent normalized shunt admittance of the lossy diaphragm:

$$\frac{Y_D}{Y_{10}^{\mathrm{TE}}} = \bar{Y}_D = \bar{G}_D + j\bar{B}_D. \tag{37}$$

Not surprisingly, $\bar{B}_D$ differs very little from that obtained in [4] for the lossless case. For a thin copper diaphragm with $\sigma = 5.8\times10^7$ S/m, the calculated normalized admittance $\bar{Y}_D$ is illustrated in Fig. 4 for X-band guide ($a = 2.286$ cm).

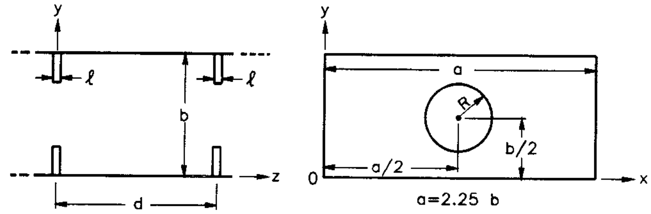

Fig 5. An X-band rectangular waveguide cavity with centered circular coupling holes in thick transverse diaphragms

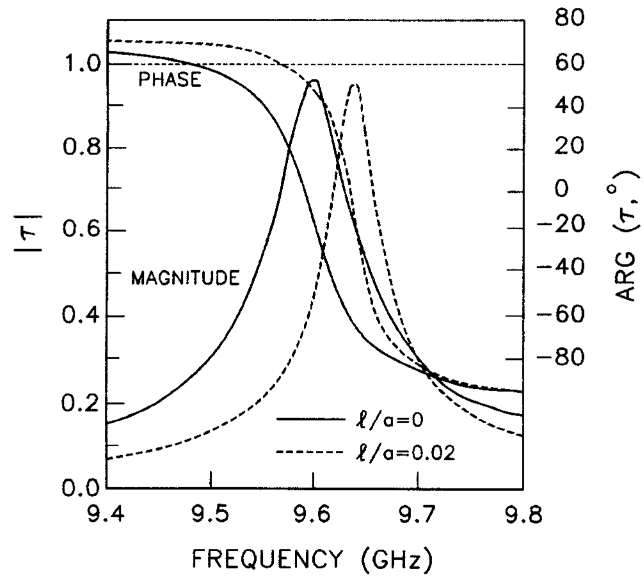

Fig. 6. Transmission coefficient τ versus frequency for a rectangular X-band cavity of length $d = 2.0$ cm with iris radius $R = 3b/8$ and wall conductivity of $\sigma = 5.8\cdot10^6$ S/m (copper).

We next consider the case of a copper rectangular X-band waveguide cavity formed by two identical diaphragms spaced 2.0 cm apart, as shown in Fig. 5. The rather large centered circular holes are of radius $R = 3b/8$. Fig. 6 provides the computed transmission coefficient τ through the cavity as a function of frequency for the zero-thickness diaphragm case ($l = 0$) and for a "thick" diaphragm ($l = 0.02b$). In both cases there is relatively little insertion loss at resonance but the thicker diaphragm with *larger* $\bar{B}_D$ has raised the resonant frequency, narrowed the bandwidth, and increased the insertion loss slightly.

The loss is more pronounced for a radius $R = b/4$; the diaphragms each provide a reflection coefficient for the TE_{10} mode of 0.998. The transmission coefficients τ for both the loss and the no loss case are given in Fig. 7. At resonance the insertion loss for the former is 1.6 dB.

Finally, we turn to a one-port cavity resonator formed by short-circuiting one end of a rectangular X-band guide and inserting a diaphragm with a centered circular hole at a distance $d = 2.0$ cm from the short, as shown in Fig. 8. Collin [5, pp. 329–336] uses a transmission line model to

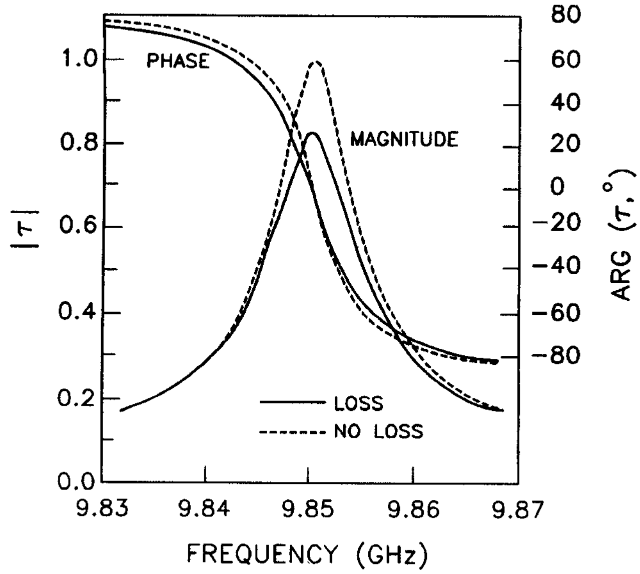

Fig. 7. Transmission coefficient τ versus frequency for loss and no loss cases. The X-band rectangular cavity is of length $d = 2.0$ cm with iris radius $R = b/4$. The diaphragm is infinitely thin.

analyze the structure. With a shunting reactance due to the diaphragm $\overline{X}_L(\beta)$, calculated from the small hole theory [5, pp. 190–194], the resonance propagation constant β_0 satisfies

$$\overline{X}_L(\beta_0) = \frac{8R^3\beta_0}{3ab} = -\tan(\beta_0 d). \tag{38}$$

Moreover, the cavity has a normalized input impedance

$$\overline{Z}_{\rm in}(\omega) = \frac{-j\overline{X}_L^2(\beta_0)}{\beta_0' d(\omega - \omega_0 - j\omega_0/2Q)} \tag{39}$$

for $\omega \simeq \omega_0$ and $\beta_0' = d\beta/d\omega$ at $\omega = \omega_0$. In (39) Q is the unloaded Q for a *completely closed* rectangular cavity with wall losses [5, p. 325].

For the 2 cm cavity and for the case of critical coupling when $\overline{Z}_{\rm in}(\omega_0) = 1$ at resonance it turns out that

$$\overline{X}_{L0} = \sqrt{\frac{\omega_0 \beta_0' d}{2Q}} = 0.0187 \qquad (\text{if } d = 2.0 \text{ cm}) \tag{40}$$

and corresponds to an aperture radius of $R = 0.2155b$ and an unloaded Q of 7840. The magnitude and phase of the resonator's reflection coefficient ρ, as deduced from $\overline{Z}_{\rm in}(\omega)$ for critical coupling, is plotted in Fig. 9, where we see that resonance occurs at 9.9233 GHz.

Using the present full-wave CCPT analysis, the radius R of the diaphragm's circular hole was varied numerically until the critical coupling value $R = 0.2032b$ was found. A plot of the resonator's reflection coefficient ρ for this case (using the full-wave CCPT) is also shown in Fig. 9. A higher resonance frequency of 9.9295 GHz is noted and is due to the slightly smaller aperture. The narrower bandwidth indicates a higher unloaded Q. For critical coupling $Q = 2Q_L = 2f_0/\Delta f$, where Δf is the 3 dB bandwidth. In our present case we calculate an unloaded Q of 10 800, much larger than the $Q = 7840$ used in the simple trans-

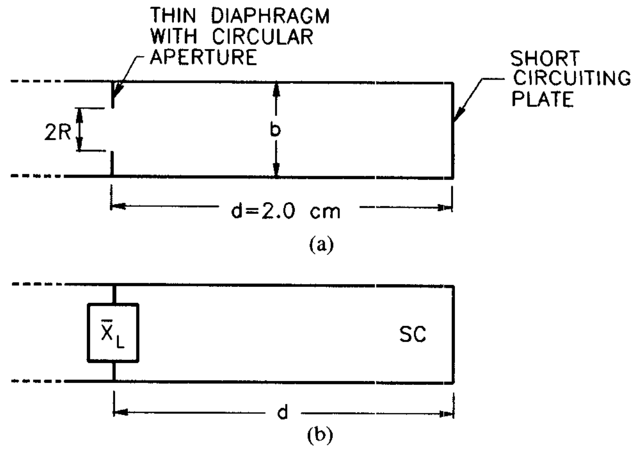

Fig. 8. (a) An X-band cavity resonator with a centered circular coupling aperture of radius R. (b) The transmission line equivalent circuit.

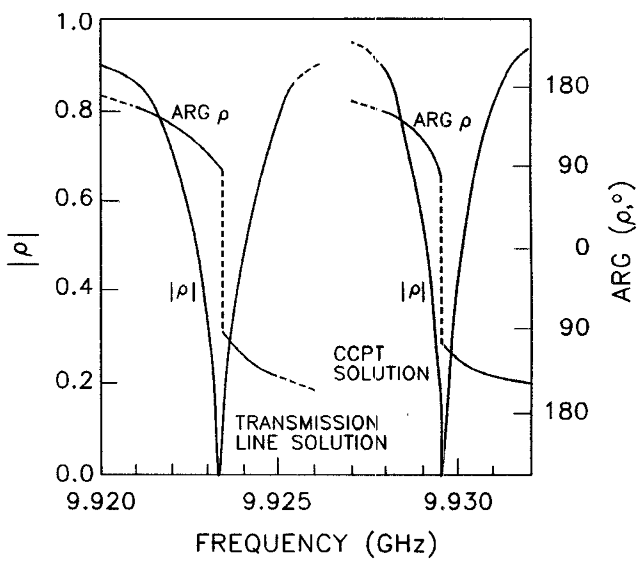

Fig. 9. Reflection coefficient ρ versus frequency for the X-band cavity resonator of Fig. 8.

mission line theory. This is probably because the latter Q does not include the stored energy of the higher order modes that exist in the neighborhood of the circular aperture and because the CCPT solution neglects the losses of these modes.

VIII. Conclusions

This paper has extended the conservation of complex power technique (CCPT) to include the effects of the large but not infinite conductivities of the transverse metallic surfaces at waveguide junctions. Incorporating the surface impedance Z_m, the resulting expressions for the scattering matrices of such lossy junctions are necessarily more complex than those for the lossless case. Nevertheless they can be straightforwardly implemented in computer code. The numerical examples that we have presented for the cases of X-band cavity resonators with circular coupling holes confirm the validity of this extension of the CCPT. Moreover it is important to remark that this formulation that has resulted in the expressions for the lossy junction's scattering matrix $[S]$ (see equations (27)–(30)) is *general* and applicable to a wide variety of waveguide scattering problems.

Appendix
The Relation Between $[W]$ and $[M]$

The matrix $[W]$ of Section III has as its mnth element

$$W_{mn} = \int_W e_{2m} \cdot e_{2n} \, ds \tag{A1}$$

$$= \int_{S_2} e_{2m} \cdot e_{2n} \, ds - \int_{S_1} e_{2m} \cdot e_{2n} \, ds \tag{A2}$$

since the aperture A is also the cross section S_1 of guide 1.

Over S_1 we can expand e_{2m} in terms of the complete set of modal functions e_{1q} in guide 1:

$$e_{2m} = \sum_q M_{mq} e_{1q} \tag{A3}$$

where M_{mq} is defined by (12). Using this modal expansion for both e_{2m} and e_{2n} in (A2), together with the orthogonality property of e_{2m} over S_2, we can immediately rewrite (A2) as

$$W_{mn} = \delta_{mn} - \sum_q \sum_r M_{mq} M_{nr} \int_{S_l} e_{1q} \cdot e_{1r} \, ds. \tag{A4}$$

Orthogonality of the e_{1q} functions over S_1 allows us to rewrite (A4) as

$$W_{mn} = \delta_{mn} - \sum_q M_{mq} M_{nq} \tag{A5}$$

which, in matrix form, is given by (22) of Section V.

References

[1] R. Safavi-Naini and R. H. MacPhie, "On solving waveguide junction scattering problems by the conservation of complex power technique," *IEEE Trans. Microwave Theory Tech.*, vol. MTT-29, pp. 337–343, Apr. 1981.

[2] ____, "Scattering at rectangular-to-rectangular waveguide junctions," *IEEE Trans. Microwave Theory Tech.*, vol. MTT-30, pp. 2060–2063, Nov. 1982.

[3] E. M. Sich and R. H. MacPhie, "The conservation of complex power technique and *E*-plane step-diaphragm junction discontinuities," *IEEE Trans. Microwave Theory Tech.*, vol. MTT-30, pp. 199–201, Feb. 1982.

[4] J. D. Wade and R. H. MacPhie, "Scattering at circular-to-rectangular waveguide junctions," *IEEE Trans. Microwave Theory Tech.*, vol. MTT-34, pp. 1085–1091, Nov. 1986.

[5] R. E. Collin, *Foundations for Microwave Engineering.* New York: McGraw-Hill, 1966.

[6] J. J. Gustincic, "A general power loss method for attenuation of cavities and waveguides," *IEEE Trans. Microwave Theory Tech.*, vol. MTT-11, pp. 83–87, Jan. 1963.

J. Douglas Wade (S'82–M'83) was born in London, Ont., Canada, in 1953. He received the B.Sc. degree in physics from the University of Toronto in 1976, the M.Sc. degree in astronomy from the University of Western Ontario in 1979, and the M.A.Sc. degree from the University of Waterloo in 1984.

In 1984 he joined the National Research Council of Canada, where he participated in the construction of a *K*-band maser receiver for the Algonquin Radio Observatory. He is presently engaged in receiver development at 345 GHz for the James Clerk Maxwell Telescope on Mauna Kea, HI.

Robert H. MacPhie (S'57–M'63–SM'79) was born in Weston, Ont., Canada, on September 20, 1934. He received the B.A.Sc. degree in electrical engineering from the University of Toronto in 1957 and the M.S. and Ph.D. degrees from the University of Illinois, Urbana, in 1959 and 1963, respectively.

In 1963, he joined the University of Waterloo, Waterloo, Ont., Canada, as an Assistant Professor in Electrical Engineering, where he is now a Professor of Electrical Engineering. His research interests currently focus on antenna arrays, waveguide scattering theory, scattering from prolate spheroid systems, and dipole antennas. During 1984–1985 he was on sabbatical leave as a professeur associé at the University of Aix-Marseille I, France, working at the Laboratoire de Radioélectricité.